

Involvement of mTORC1 and mTORC2 in regulation of glioblastoma multiforme growth and motility

NICHOLAS GULATI¹, MICHAEL KARSY^{1,2}, LADISLAU ALBERT¹,
RAJ MURALI¹ and MEENA JHANWAR-UNIYAL^{1,2}

Departments of ¹Neurosurgery and ²Experimental Pathology, New York Medical College, Valhalla, NY 10595, USA

Received March 26, 2009; Accepted May 13, 2009

DOI: 10.3892/ijo_00000386

Abstract. The AKT/mammalian target of Rapamycin (mTOR) signaling pathway plays a critical role in glioblastoma multiforme (GBM) oncogenesis due to activation of AKT. We studied two distinct complexes, mTOR complex 1 (mTORC1) and mTOR complex 2 (mTORC2), through which mTOR controls cell survival, growth and motility. Inhibition of mTOR by Rapamycin (RAPA) resulted in time-dependent suppression of S6 ribosomal protein (pS6K^{Ser235/236}; mTORC1 substrate) and caused transient suppression of pAKT^{Ser473} (mTORC2 substrate) at 1 to 3 h followed by a consistent increase from 6 to 24 h. Inhibition of mTOR or phosphoinositide 3-kinase (PI3K) suppressed platelet-derived growth factor (PDGF)- or fibronectin (FN)-induced activation of p70S6K^{Thr389}. Combined inhibition of mTOR and PI3K abolished PDGF- or FN-induced activation of STAT3^{Ser727}. Expression of pAKT was suppressed by siRNA silencing of mTORC2 co-protein Rictor, but not by mTORC1 co-protein Raptor. GBM cell proliferation and motility paralleled the activation of mTORC2. Combined inhibition of mTOR and PI3K had an additive effect on suppressing cell growth and motility. PDGF-induced nuclear localization of mTOR was blocked by pre-treatment with RAPA. The results demonstrated that an activation of mTORC2 occurs when mTORC1 is inhibited by RAPA. Therefore, simultaneous suppression of mTORC1 and mTORC2 may provide novel therapy for GBM.

Introduction

Glioblastoma multiforme (GBM), a grade IV astrocytoma, is the most common primary brain tumor in humans and despite current treatment modalities such as surgical resection,

radiotherapy and chemotherapy, median survival time remains ~1 year after diagnosis (1). GBM may develop *de novo* (primary GBM) or progress from a low-grade or anaplastic astrocytoma (secondary GBM) with either type defined by specific clinical courses (2). Multiple genetic pathways are abnormal in GBM including amplification of epidermal growth factor receptor (EGFR), loss of chromosome 10q, mutation in phosphatase and tensin homolog (PTEN), mutation of p53, and concomitant loss of p16 and p18 (2,3). Furthermore, aberrant signaling pathways contributing to abnormal cell migration, invasion and proliferation are responsible for the aggressive nature of GBM. Parallels between growth factor signaling elements implicated in GBM progression and those that control crucial stages in neural development are consistent with recent evidence signifying neural stem and/or progenitor cells as the cell type of origin for GBM (4-6). Furthermore, the stem cell marker nestin and JNK in tumor and peri-tumor areas served as prognostic markers for GBM (7).

Mutations of tumor suppressor PTEN that occur with an estimated frequency of 70-90% and its associated downstream proteins, are well accepted changes with potent influences on GBM function (8,9). A loss of PTEN increases the pool of self-renewing neural stem cells and induces loss of homeostatic control of proliferation indicating cell cycle dysregulation during gliomagenesis (10). PTEN loss results in the up-regulation of the phosphoinositide 3-kinase (PI3K)/AKT pathway involved in regulation of cellular processes such as transcription, translation, cell cycle progression and apoptosis (11,12). AKT (protein kinase B), a serine/threonine protein kinase, regulates cell growth and survival by activating multiple downstream targets, including GSK-3B, p21, p27 and NF-κB (11) and activation of AKT plays a crucial role in gliomagenesis as shown in animal models (13).

Notably, the downstream signaling target of AKT, mammalian target of Rapamycin (mTOR), is a critical effector of cell signaling pathways generally deregulated in many cancers including GBM (14-16). Recent studies have suggested that mTOR exists in two multiprotein complexes, mTOR complex 1 (mTORC1) and mTOR complex 2 (mTORC2) (15). mTORC1 and mTORC2 are two structurally and functionally distinct protein complexes which share the catalytic subunit of the protein kinase mTOR (17). In mTORC1, mTOR is associated with Rapamycin-sensitive adapter protein of mTOR (Raptor) whereas in mTORC2, mTOR is associated with Rapamycin-insensitive companion of mTOR (Rictor) (16).

Correspondence to: Dr Meena Jhanwar-Uniyal, Departments of Neurosurgery and Experimental Pathology, New York Medical College, Valhalla, NY 10595, USA
E-mail: meena_jhanwar@nymc.edu

Key words: mammalian target of Rapamycin, glioblastoma multiforme, AKT, Rapamycin-sensitive adapter protein of mTOR, Rapamycin-insensitive companion of mTOR

mTOR activation enhances RNA translation via S6 ribosomal protein (18). Upstream of mTORC1 and mTORC2, the GTPase termed Ras homolog enriched in brain (Rheb) is found to activate mTORC1 via direct binding to mTOR (19). Activation of upstream AKT inhibits the Tuberculin Sclerosis 1/2 (TSC 1/2) complex that allows Rheb to activate mTORC1 (16). Downstream of mTORC1, the kinase S6K1 directly phosphorylates multiple targets including programmed cell death protein 4 (PDCD-4), a tumor suppressor (20). Among multiple feedback loops, the negative regulation of AKT activity by mTORC1 is largely attributed to the effect of S6K1 generating inhibitory phosphorylation of insulin receptor substrate-1 (IRS-1) thus reducing PI3K activation (21). Some studies have indicated that it is unlikely that this is the only mechanism by which activated mTOR leads to the inhibition of AKT, since AKT inhibition by mTORC1 also has been observed in the presence of several growth factors and not exclusively in the presence of IGF-1 (22).

The transcription factor Signal Transducer and Activator of Transcription 3 (STAT3) is known to play an important role in astrocyte differentiation during normal brain development (23). As with mTOR, STAT3 is present downstream of EGFR. It appears that STAT3 activation by mTOR occurs at mTOR-specific phosphorylation of STAT3 at serine 727 (24). Cytokine-induced STAT3 activation is specifically disrupted in PTEN-deficient but not PTEN-expressing GBM cells (25). Furthermore, activation of STAT3 in GBM tumors may indicate enhanced proliferation (26). However, the involvement of STAT3 in gliomagenesis via the mTOR-stimulated pathway remains to be established.

Several tumors and familial syndromes show mutations along the PI3K/AKT/mTOR pathway, thus creating the potential for novel chemotherapeutic approaches to control or abate tumorigenesis (27). Clinical trials of Rapamycin (RAPA) and its analogs (CCI-779/temsirolimus, RAD001/everolimus, AP23573) have shown great promise in a variety of tumor treatments, but have also created new challenges regarding drug resistance in the treatment of GBM. Two recent phase II trials of temsirolimus treatment in GBM showed a partial response with a median time to progression of 2.3 months (28,29). Despite significant therapeutic advances, GBM remains incurable in these treatments. Moreover, drugs that inhibit both mTOR and PI3K have enhanced activity in GBM models (30). Thus far, the molecular mechanisms of drug failure have not been fully understood. Consequently, the primary aim of this study is to decipher a shift between mTORC1 and mTORC2 and delineate the consequence of this mechanism as it pertains to cellular growth and motility of GBM.

Materials and methods

Cell lines. GBM cell lines LN-18 and U373 (ATCC, Manassas, VA) were used to investigate the involvement of the PI3K/AKT/mTOR signaling pathway in GBM progression.

Cell culture. Cell lines were maintained in DMEM (Invitrogen, Carlsbad, CA) supplemented with 10% FBS and 1% penicillin/streptomycin/amphotericin in a humidified 5% CO₂ incubator at 37°C. Cells were made quiescent by serum deprivation 24 h

prior to treatment with various combinations of Rapamycin (RAPA, mTOR inhibitor), LY294002 (LY, PI3K inhibitor), platelet-derived growth factor (PDGF), epidermal growth factor (EGF) (EMD Chemicals, Gibbstown, NJ) or fibronectin (FN, extra-cellular matrix) (Sigma-Aldrich, St. Louis, MO).

Isolation of protein. Protein extraction was performed with whole cell lysis buffer containing 1% Triton X-100, 10 mM Tris-HCl (pH 7.5), 150 mM NaCl, 5 mM EDTA, phosphatase and protease inhibitors (Sigma-Aldrich). Protein concentrations were determined by the modified Lowry Method (Bio-Rad Laboratory, Hercules, CA).

Western blot analysis. Equal amounts of protein were resolved on a 4-16% gradient, 6%, or 10% SDS-PAGE gel and then electrotransferred onto nitrocellulose membrane. Membranes were processed according to the manufacturers' instructions (Santa Cruz Biotechnology, Santa Cruz, CA; Cell Signaling Technology, Danvers, MA) using primary antibodies for activated and total mTOR, AKT, Rictor, Raptor, ribosomal protein S6K (S6K), 70 kDa ribosomal protein S6 kinase (p70S6K) and STAT3 at 1:1000 dilutions, and bands were detected by chemiluminescence (Cell Signaling Technology). Blots were stripped with reagent (EMD Chemicals) and re-probed with actin or respective total antibodies to ensure equal loading. Experiments were conducted at least 3 times.

siRNA. Cells were transfected with siRNA according to the manufacturer's instructions (Qiagen, Valencia, CA). Small interfering RNA (siRNA) duplex target sequences were generated for: mTOR (FRAP; NM_004958; CAGGCCTATGGTTCGAGATTTA), Raptor (KIAA1303; NM_020671; CTGGGTCTTCAACAAGAATA), Rictor (NM_152756; ATGACCGATCTGGACCCATAA), and ribosomal protein S6 kinase (RPS6KB1; NM_003161; AAGCCGGAGAATATCATTCTT). AllStar Hs Cell Death Control and non-specific AllStar Negative Control (Qiagen) were used as positive and negative controls, respectively. Following 48 h incubation, proteins were collected by Western blot analysis. Successful transfection was documented by apoptotic cells (Fig. 3A).

Cell proliferation assays. Cell growth was measured by MTT assay according to the manufacturer's protocol (Chemicon, Billerica, MA). Cells (3,000/well) were seeded onto a 96-well plate and made quiescent for 24 h prior to treatment. After completion of treatment, fresh media containing 10 μ l of MTT reagent was added to cells, plates were incubated at 37°C for 4 h, 100 μ l of detergent reagent was added and absorbance was measured after 2 h.

Radial migration assay. A monolayer radial migration assay technique was used to determine the GBM motility (31). Ten individual 7-mm circular areas (CSM, Phoenix, AZ) were coated with 10 μ g/ml laminin and 0.1% BSA (Sigma-Aldrich). Cells were seeded (3,000 cells/ μ l) via a CSM manifold onto the circular areas. After overnight incubation, the manifold was removed, cells were treated with various drugs (EGF, LY, RAPA) or RAPA-timed treatments. Initial and 24 h post-treatment cell radii were recorded using an inverted microscope (Axiovert 100M; Zeiss, Thornwood, NY).

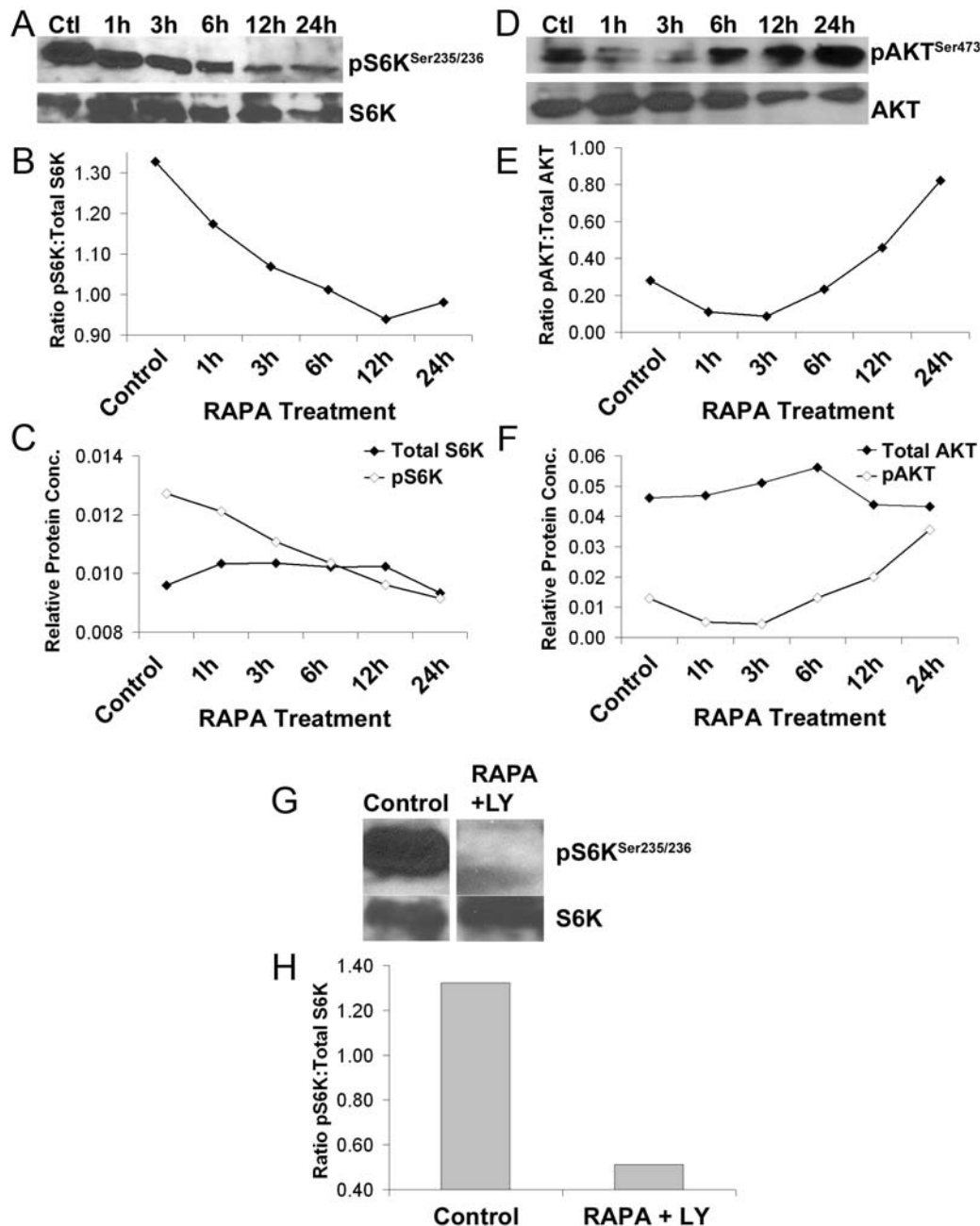


Figure 1. Timed Rapamycin (RAPA) treatment induces shift between mTORC1 and mTORC2 complexes. Western blot analysis demonstrating the time course of pS6K^{Ser235/236} and pAKT^{Ser473} following RAPA (10 nM) treatment. (A) Ribosomal protein pS6K expression declined over 24 h following RAPA treatment. A moderate decline in pS6K was evident at 1 and 3 h, followed by a substantial time-dependent decline in S6K activation between 6 to 24 h. The same blot was stripped and reprobbed for total S6K expression showing invariable expression across treatment. (B) The ratio of pS6K vs. total S6K graphed against time demonstrated a time-dependent drop (1 to 12 h) following RAPA treatment. (C) A graph of pS6K and total S6K values separately plotted against time demonstrated a persistent decline in pS6K through 24 h whereas levels of total S6K remained invariable. (D) Western blot analysis shows the time course of pAKT^{Ser473} following RAPA (10 nM) treatment. After an initial decline in pAKT levels from 1 to 3 h, a consistent increase in AKT activation was evident at 6, 12 and 24 h. The same blot was stripped and reprobbed with total AKT showing invariable expression across treatments. (E) Densitometric analysis of the pAKT:total AKT ratio shows an initial drop followed by a persistent increase. (F) Independent values of pAKT and total AKT are plotted. An alteration in pAKT levels following RAPA treatment represents the ratio seen in (E), since total AKT remained invariable throughout 24 h. (G) Western blot analysis shows the expression of pS6K and total S6K following combined 24 h treatment with RAPA (10 nM, mTOR inhibitor) and LY (10 μ M, PI3K inhibitor). Combined treatment totally suppressed the levels of pS6K. The same blot was stripped and reprobbed with total S6K showing invariable expression compared to control. (H) Densitometric analysis of pS6K:total S6K expression showed that compared to control, the levels after combined treatment were dramatically suppressed.

Migration rate was calculated by Scion Image (Scion, Frederick, MD) and migration distance was calculated by Axiovision (Zeiss).

Chemotactic migration. Directional migration was performed using a 48-well modified Boyden chamber kit (NeuroProbe,

Gaithersburg, MD). Quiescent cells were subjected to RAPA-timed treatments (1, 3, 6, 12, 24 h). Vehicle-treated cells served as controls. Cells were aliquoted (3,000 cells/ μ l) in either serum-free media or their respective RAPA-treated media. FN (20 ng/ml, Sigma-Aldrich) was used as a chemo-attractant and cells were allowed to migrate for 4 h through a

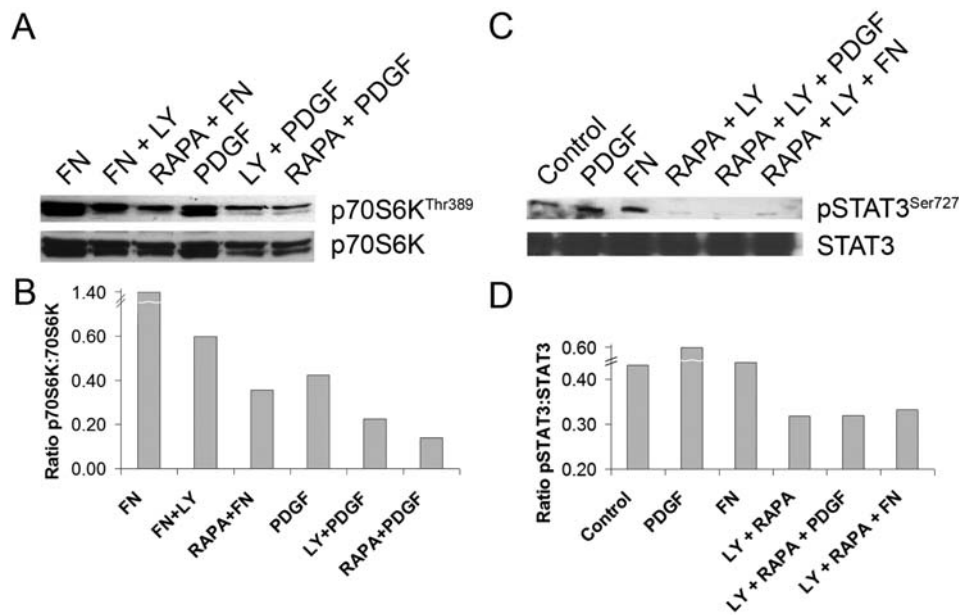


Figure 2. PDGF- or FN-induced activation of p70S6K^{Thr389} and STAT3^{Ser727} was abrogated by PI3K and/or mTOR inhibition. (A) Activation of p70S6K^{Thr389} (mTOR-sensitive site) showed a dramatic increase following FN (20 ng/ml) or PDGF (25 ng/ml) treatment. Treatment with rapamycin (RAPA; 10 ng/ml) or LY294002 (LY; 10 μ M) for 24 h prior to treatment with PDGF or FN for 30 min caused a marked decline in pp70S6K expression. The same blot was stripped and re-probed for p70S6K which represents an unaltered expression with all treatments. (B) pp70S6K:total p70S6K ratio is presented for each treatment and shows that either RAPA or LY abrogated PDGF- or FN-induced activation of p70S6K. (C) Expression of pSTAT3^{Ser727} (an mTOR-sensitive site) was increased by PDGF treatment as compared to control (vehicle) or FN. Combined pre-treatment with mTOR (RAPA, 10 nM) and PI3K (LY, 10 μ M) inhibitors not only totally abolished the activation of STAT3 but also suppressed the activation of STAT3 by PDGF or FN. The same blot was stripped and re-probed with total STAT3 showing an equal expression across treatments. (D) The densitometric analysis of pSTAT3 vs. STAT3 reflects the findings described above.

PVC membrane (8 μ m pore). The membrane was fixed in 70% ethanol, scraped along the non-migrated cell surface and stained with DiffQuick (IMEB, San Marcos, CA). Migrated cells were imaged at 2.5X (Axiovert 100M) and analyzed as a percentage of total microscopic field occupied by migrated cells (ImageJ, NIH, Bethesda, MD).

Immunofluorescence. Quiescent cells were treated with RAPA (10 nM), PDGF (25 ng/ml), or RAPA and PDGF followed by fixation with 4% paraformaldehyde/0.1% Tween. Cells were blocked with 5% BSA, incubated for 1 h with mTOR antibody (1:50, FRAP H-266, Santa Cruz Biotechnology) and subsequently incubated with fluorescein-conjugated antibody (Jackson ImmunoResearch, West Grove, PA). DAPI counterstain was performed (Sigma-Aldrich).

Statistics. Values are presented as the mean \pm SEM. Student's t-test (unpaired, two-tailed) was used to evaluate significant variations between control and treated groups. T-values of $p < 0.05$ were considered significant while $p < 0.10$ was defined as a trend towards significance.

Results

RAPA treatment induces shift between mTORC1 and mTORC2 complexes. mTOR is present in two complexes, mTORC1 and mTORC2. mTORC1 activity is determined by phosphorylation of p70S6K^{Thr389} or ribosomal subunit S6K^{Ser235/236} and mTORC2 activity can be measured by pAKT^{Ser473}. To investigate the shift between the two complexes, we analyzed the phosphorylation of S6K and AKT after timed treatments with RAPA (10 nM) between 1 to 24 h. RAPA caused a time-dependent drop in

S6K phosphorylation over the course of 1 to 12 h and plateaued at 24 h. Blots were also re-probed for total S6K antibody (bottom panel; Fig. 1A). Densitometric quantification of pS6K:total S6K ratio demonstrated a persistent decline in S6K activity over 12 h (Fig. 1B). Also shown are the values of pS6K and total S6K separately against time, which represent that the decline in pS6K:S6K ratio was due to the decline in pS6K levels (Fig. 1C).

AKT phosphorylation at Ser473 showed a different pattern following timed RAPA treatment. An initial suppression in pAKT was observed at 1 to 3 h, followed by a consistent upregulation of AKT activation at 6, 12 and 24 h (Fig. 1D). Densitometric analysis of pAKT:total AKT ratio demonstrated a 3-fold decline from control to 3 h followed by an increase of 9-fold thereon up to 24 h (Fig. 1E). Levels of pAKT reflect this ratio since total AKT levels remained invariable across treatments (Fig. 1F). In addition, there was a correlation between pAKT:AKT and pS6K:S6K from 1 to 3 h ($r = 0.95$) and an inverse correlation from 3 to 12 h ($r = -0.99$).

When cells were treated with combined inhibitors of mTOR (RAPA; 10 nM) and PI3K (LY; 10 μ M) for 24 h, there was total suppression of pS6K (Fig. 1G). Densitometric analysis showed a 61% decline in pS6K:total S6K ratio from control (Fig. 1H).

PI3K and/or mTOR inhibition curtails PDGF or FN-induced activation of p70S6K^{Thr389} and STAT3^{Ser727}. Treatment with FN or PDGF induced phosphorylation of p70S6K^{Thr389} (an mTOR-sensitive site). Pre-treatment with RAPA (10 nM) or LY (10 μ M) for 24 h prior to treatment with FN or PDGF (30 min) caused a noticeable suppression of p70S6K phosphorylation (Fig. 2A). The same blot was re-probed with

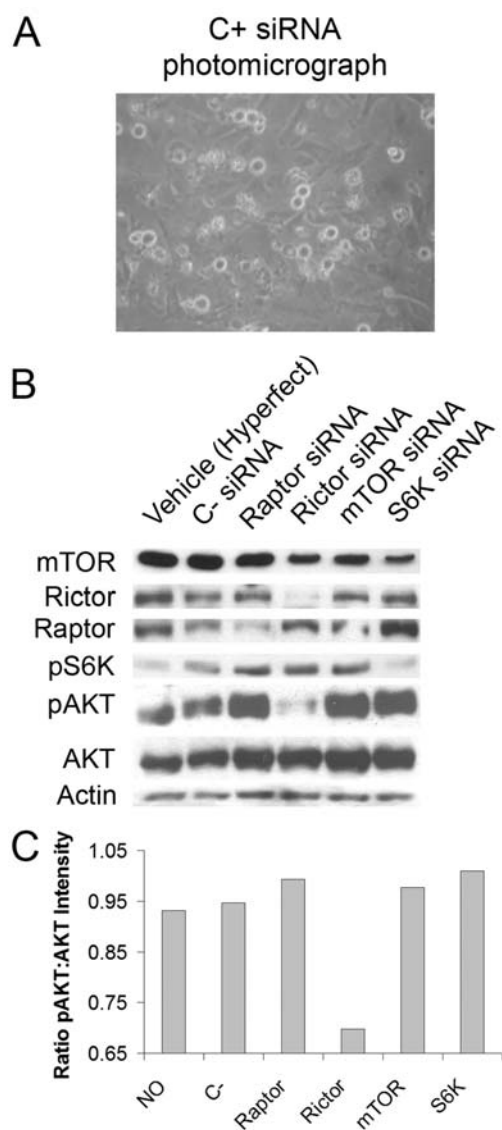


Figure 3. Activation of AKT occurs by inhibition of siRNA silencing of mTORC1 but not mTORC2. Protein synthesis of mTOR, Raptor, Rictor and S6K was inhibited via siRNA treatments for 48 h and AKT activation was determined. (A) Positive control siRNA, AllStar Hs Cell Death Control, displayed apoptotic cells indicating a successful transfection. (B) Protein expression of mTOR, Raptor, Rictor and ribosomal protein S6K was performed 48 h after siRNA treatment. Raptor, Rictor and p70S6K showed complete suppression after respective treatments, however mTOR siRNA was partially effective in reducing its expression. (C) Activated AKT (pAKT^{Ser473}) was analyzed in mTOR, Raptor, Rictor and S6K siRNA-treated cells and showed that only Rictor siRNA inhibited pAKT expression, suggesting that pAKT is downstream of mTORC2. Densitometric analysis of pAKT:total AKT levels reflects this latter finding.

total p70S6K. The ratio of pp70S6K:total p70S6K showed that RAPA or LY treatment suppressed PDGF- or FN-induced phosphorylation of p70S6K (Fig. 2B).

Phosphorylation of STAT3^{Ser727} (an mTOR-sensitive site) was induced by PDGF or FN treatment. A combined pre-treatment with RAPA (10 nM) and LY (10 μ M) for 24 h prior to PDGF or FN treatment, completely suppressed STAT3 phosphorylation (Fig. 2C). The same blot was stripped and reprobed for total STAT3 and showed constant levels of total STAT3 across treatments. The ratio of pSTAT3:total STAT3 demonstrated that PDGF- or FN-induced phosphorylation of

STAT3 was curtailed by a combined pre-treatment with LY and RAPA.

Inhibition of mTORC2 but not mTORC1 via siRNA silencing activates AKT. Protein synthesis of mTOR, Raptor, Rictor and S6K via siRNA interference was suppressed in order to determine the activation of AKT and place it with respect to mTORC1 and mTORC2. Cells were maintained in their respective siRNA. mTOR concentration was mildly altered by its siRNA, which may be explained by the fact that this protein is nutritionally sensitive. The expression of Raptor, Rictor and ribosomal protein S6 kinase were reduced after their respective siRNA treatments (Fig. 3B). Notably, pAKT expression was reduced dramatically by Rictor siRNA but not Raptor, mTOR or ribosomal protein S6 kinase siRNA (Fig. 3C), placing AKT downstream from mTORC2.

Inhibition of mTOR or PI3K causes suppression of GBM cell proliferation in a discrete manner. In order to establish whether the mTORC1 to mTORC2 shift contributes to cell proliferation, cells were treated with RAPA at low (10 nM) and high (100 nM) doses for 12, 24 and 48 h (Fig. 4A and B). RAPA treatment for 12 h at low and high doses caused a suppression of cell viability by 28 and 47%, respectively. At 24 h there was a negligible difference in cell viability compared to control for both doses. A noticeable drop in cell viability to 74% was seen at 48 h with low dose while no viable cells were detectable at high dose. The treatment with LY, however, showed a dose- and time-dependent decline in cell numbers at both low (5 μ M) and high (10 μ M) doses of LY, $r = -0.96$ and -0.99 , respectively (Fig. 4B).

In order to establish the effects of the AKT/mTOR pathway on cell proliferation, cells were treated with PDGF or FN following 24 h of LY or RAPA pre-treatments. RAPA treatment alone caused a modest decline in cell viability (68%, Fig. 4C). Pre-treatment of cells with RAPA for 24 h suppressed PDGF or FN response to cell proliferation. LY pre-treatment caused a noticeable suppression of PDGF or FN response to cell viability (Fig. 4D). Combined treatment with RAPA and LY noticeably suppressed PDGF induced cell growth ($p < 0.05$, Fig. 4E).

Inhibition of PI3K suppresses GBM cell motility and mTOR suppression influences GBM motility via mTORC2. Two methods of migration were used in this study: i) random, non-directional migration on laminin and ii) directional migration towards a chemoattractant (FN) using a modified Boyden chamber. For analysis of radial migration following drug treatments, the radial migration rate was calculated according to the farthest traveled cell over a 24 h period. A representation of the migrated cells during individual treatments is shown (Fig. 5A). EGF significantly increased cell migration 3-fold compared to control (Fig. 5B). The distances that GBM cells migrated following timed RAPA treatments are presented (Fig. 5C). Timed treatment with RAPA over a 24 h period showed that while a short-term RAPA treatment (1, 3 and 6 h) caused no alteration in cell motility compared to control, a trend towards increased GBM cell motility was evident at 12 and 24 h ($p < 0.1$, Fig. 5D). Chemotactic analysis following RAPA treatments over a

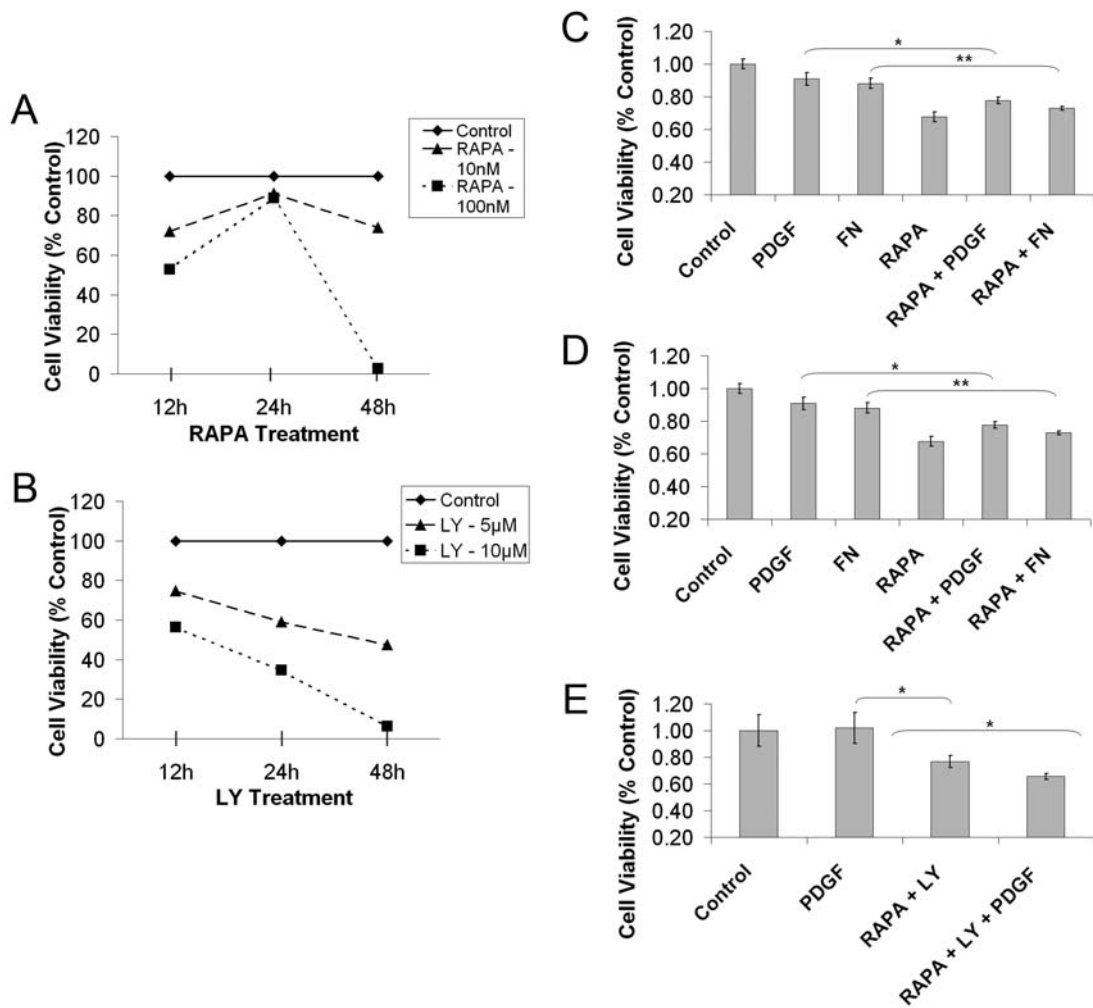


Figure 4. Effects of PI3K and mTOR suppression on GBM cell proliferation. A dose and time response of PI3K inhibitor (LY294002;LY) and mTOR inhibitor (rapamycin; RAPA) showed that cell viability was influenced in a discrete manner. Cell viability was measured using MTT assay and values were normalized to control which was set at 100. (A) While LY treatment at low (5 μ M) and high (10 μ M) -dose showed a dose- and time-dependent suppression of cell growth, (B) RAPA treatment showed a parabolic pattern of cell viability over time. (C) Pre-treatment of cells with RAPA (24 h) suppressed PDGF (24 h) or FN (24 h) response to cell proliferation. (D) LY pre-treatment caused a noticeable suppression of PDGF or FN response to cell viability. (E) A combined treatment with LY and RAPA showed an additive effect on cell growth suppression and inhibited PDGF-induced cell proliferation. Results are means with standard error of the mean. * $P < 0.05$, ** $P < 0.01$, *** $P < 0.0001$. See Results for details.

24 h time course demonstrated a lack of motility at 1 and 3 h while a significant increase in cell motility at 6 h ($p < 0.05$), 12 h ($p < 0.05$) as well as 24 h ($p < 0.05$) was observed (Fig. 5E and F). Inhibition of PI3K (LY) noticeably reduced non-directional cell migration while inhibition of mTOR (RAPA) did not alter migration rate compared to control over a 24 h period. An additional finding of this study is that when a combined inhibition of PI3K and mTOR was used, a significant trend towards suppression of cell migration was found compared to PDGF treatments ($p < 0.01$, Fig. 5G).

PDGF-induced nuclear localization of mTOR is suppressed by RAPA treatment. mTOR may exert its action via cytoplasmic-nuclear shuttling. Under vehicle-treated condition, mTOR was predominantly localized to the cytoplasm as seen by the sharp staining of mTOR in the cytoplasm (Fig. 6A). We examined whether PDGF (25 ng/ml) influenced the signaling of mTOR through nuclear localization. When quiescent GBM cells were treated with PDGF for 30 min, nuclear localization of mTOR protein was observed. This

nuclear localization was blocked by pre-treatment of cells with RAPA (10 nM) showing only cytoplasmic mTOR localization. These results indicate that PDGF-induced mTOR localization was influenced by RAPA.

Discussion

Our results demonstrated a significant contribution of mTORC2 in controlling GBM cell growth and motility. The findings showed that RAPA (mTOR inhibitor) caused sustained decline in pS6K and enhanced AKT activity over a period of 24 h. Activation of p70S6K or STAT3 was suppressed by inhibition of PI3K or mTOR. siRNA silencing of Rictor, but not Raptor, mTOR or S6K, suppressed activation of AKT. Inhibition of either PI3K or mTOR suppressed cell growth and in combination they had an additive effect. PI3K inhibition caused a dose- and time-dependent suppression of cell growth, while a parabolic curve of cell proliferation was obtained with mTOR inhibition. Both directional and non-directional migration increased with sustained mTOR

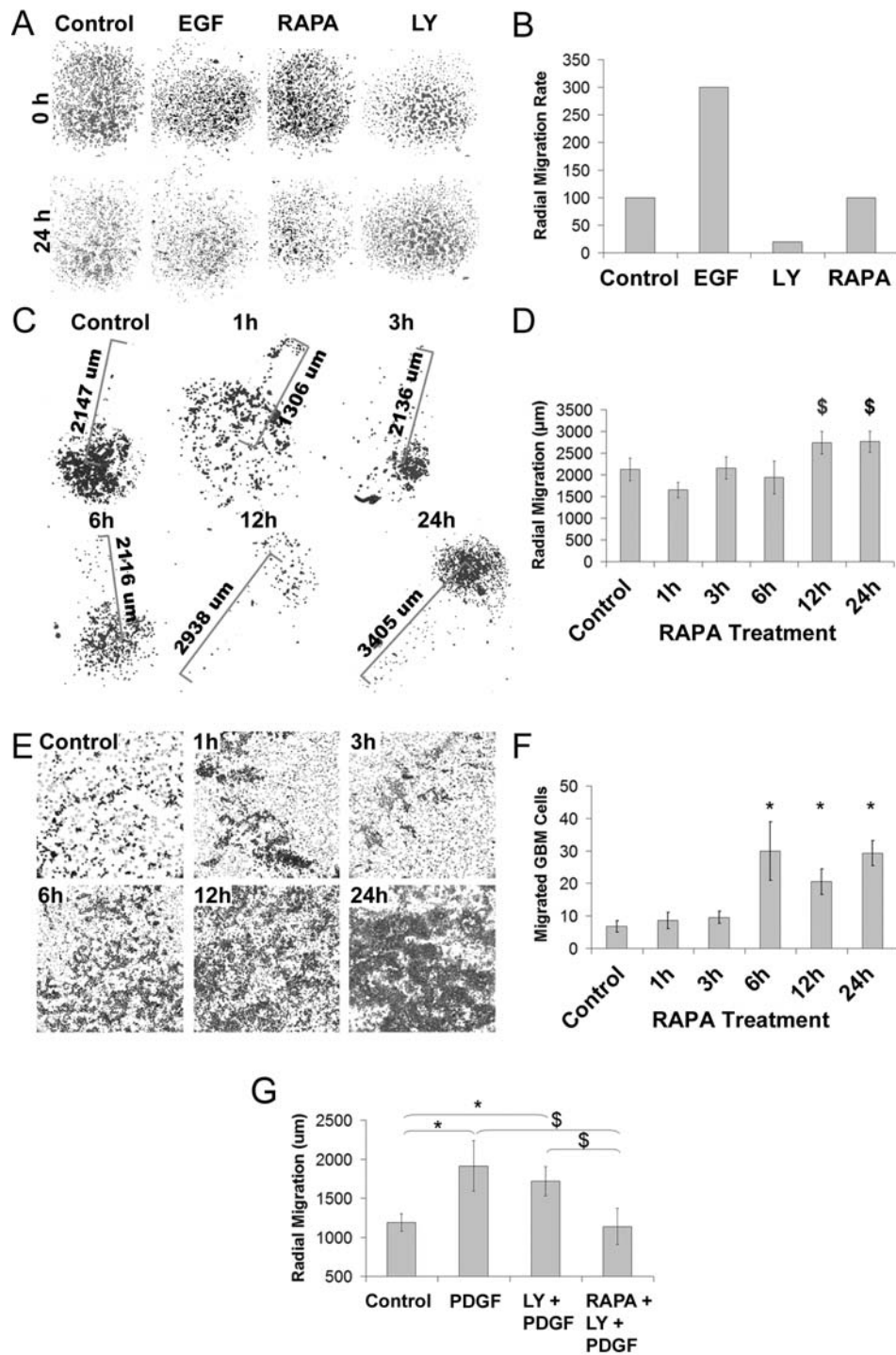


Figure 5. Effects of PI3K and mTOR suppression on GBM directional and non-directional migration. Non-directional migration rate (A) imaged and (B) calculated over a period of 24 h indicated that LY 294002 (LY) but not rapamycin (RAPA) showed a dramatic suppression in migration. EGF treatment showed a marked increase in migration rate. The mTORC2 influenced GBM cell migration in a RAPA-dependent manner. (C) Photomicrographs (x2.5) and (D) quantification of non-directional migration distance following timed-RAPA treatment showed that while no significant change was observed following 1, 3 and 6 h of RAPA treatment, a trend towards increased cell migration was seen at 12 and 24 h. Similarly, (E) photomicrographs (x10) and (F) quantification of the number of migrated cells (as percent of surface area) studied by directional migration towards FN showed no alteration in migration at 1 and 3 h compared to control, but a robust increase was observed at 6, 12 and 24 h. (G) While pre-treatment with LY suppressed PDGF-induced non-directional GBM migration, a combined treatment with LY and RAPA showed a trend towards an additive effect in suppressing cell migration. Results show mean with standard error of mean. * $P < 0.10$, $^{\$}P < 0.05$. See Results for details.

inhibition; however, PI3K inhibition more effectively suppressed non-directional migration. Inhibition of mTOR influenced its PDGF-induced cytonuclear shuttling.

We demonstrated that suppression of mTOR led to a time-dependent decrease in pS6K^{Ser235/236} up to 12 h with no

significant change from 12 to 24 h (Fig. 1A and B). Suppression of S6K downstream from mTORC1 occurs since RAPA dissociates the binding of Raptor with mTOR (16). Activation of AKT showed a different pattern, where pAKT levels were suppressed for the initial 1-3 h of mTOR inhibition

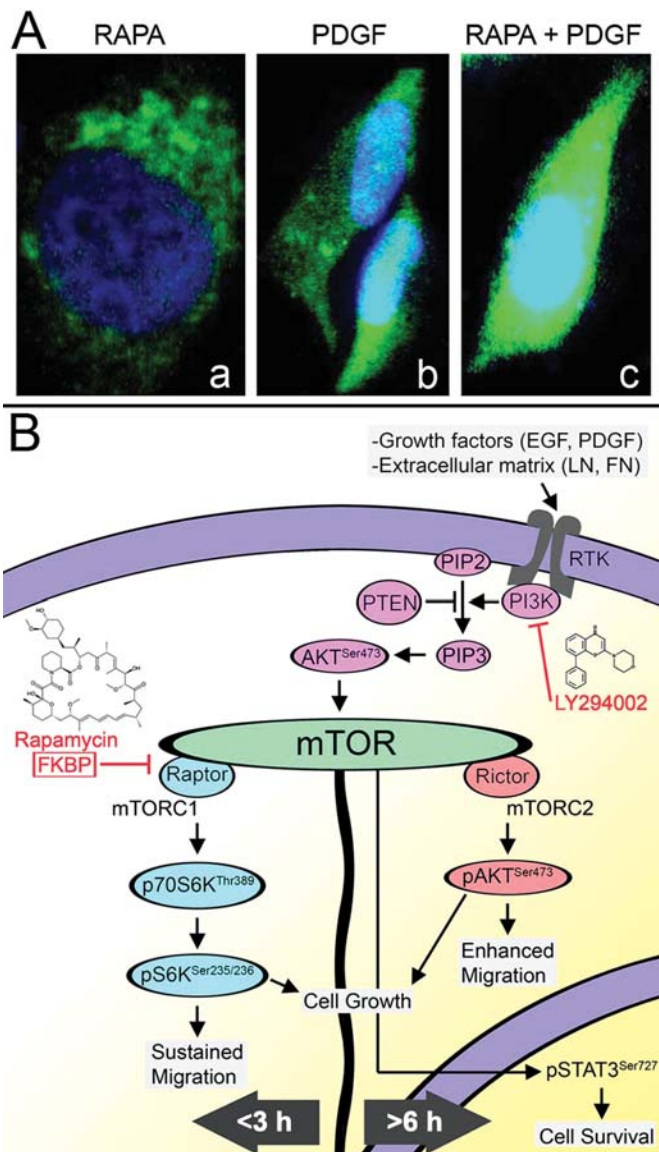


Figure 6. (A) Nuclear localization of mTOR; and (B) signaling pathways involving mTORC1 and mTORC2. (A) a) mTOR expression is evident in the cytoplasm of rapamycin (RAPA)-treated GBM cells; b) upon stimulation by PDGF, mTOR expression was seen in both the nucleus and cytoplasm; and c) pre-treatment with RAPA attenuates PDGF induced nuclear expression of mTOR. (B) A schematic representation of our findings are presented depicting a shift between mTORC1 and mTORC2 following RAPA treatment. Short-term RAPA treatment (<3 h) reduced S6K^{Ser235/236} activation leading to a suppression of cell growth and sustaining cell motility, whereas RAPA treatment (>6 h) shifts to mTORC2 activity, resulting in enhanced cell growth and motility. A combined inhibition of mTOR (RAPA) and PI3K (LY294002) completely abolished S6K^{Ser235/236} expression and also abrogated activation of pSTAT3^{Ser727} induced by PDGF or FN treatment. Indication of a 'p' before any protein shows that the protein is phosphorylated/activated. EGF, epidermal growth factor; PDGF, platelet-derived growth factor; LN, laminin; FN, fibronectin; RTK, receptor tyrosine kinase; PI3K, phosphoinositide 3-kinase; PIP2, phosphatidylinositol bisphosphate; PIP3, phosphatidylinositol (3,4,5)-trisphosphate; PTEN, phosphatase and tensin homolog; mTOR, mammalian target of Rapamycin; Raptor, rapamycin-sensitive adapter protein of mTOR; Rictor, rapamycin-insensitive companion of mTOR; FKBP, STAT3; Signal Transducers and Activator of Transcription 3.

but gradually increased from 6-24 h. The latter finding suggests an activation of mTORC2 where mTOR forms a complex with Rictor upon disengaging from Raptor. This finding may be explained by one of the following two mechanisms: i)

activation of a negative feedback loop due to a drop in S6K levels below threshold leading to an activation of AKT via an upstream IRS-1 (32), or ii) activation of mTORC2 complex from a shift to mTORC2 formation instead of mTORC1 as a result of disruption in Raptor binding. Our findings suggest that the activation of pAKT at later time points following RAPA treatment was due to the activation of mTORC2, since silencing of Rictor but not Raptor regulated pAKT levels (Fig. 3B and C). The observation of a sustained decline in pS6K expression suggests that RAPA treatment continues to influence mTORC1 activity up to 24 h. Some studies have demonstrated that prolonged treatment with RAPA or its derivatives reduce mTORC2 signaling and inhibit AKT activation in cancer cells (33). An increase in activated AKT expression has been seen in clinical trials of everolimus (RAD001), an analog of RAPA, on a variety of solid tumors (34). Studies done on mouse models of GBM have shown that the effects of oncogenic AKT or Ras on gene expression are via the selective induction of mRNA translation regulating growth, transcriptional regulation, cell-cell interaction and morphology (35). Moreover, genetic and biochemical experiments have indicated that AKT can activate mTORC1 via the direct activation of mTORC2 (11,36). As with our study, AKT phosphorylation appears to be induced by the activation of mTORC2 (26,37). Future studies would emphasize the consequence of AKT activation via mTORC2. By demonstrating an inadvertent activation in AKT after mTOR inhibition, a potential mechanism for the drug resistance following treatment with RAPA or its analogs currently in clinical trials can be explained.

mTOR resides in two multiprotein complexes, with mTORC1 regulating cell growth and translation initiation, while mTORC2 is involved in cytoskeletal reorganization (16). The induction of mRNA translation by mTORC1 is mediated by the interaction of downstream S6K and the eukaryotic translation initiator factor 4E-BP1. S6K can inhibit AKT through a feedback loop via IRS-1 (11) thus physiologically low levels of S6K are considered tumorigenic (26). However, the threshold level of S6K that becomes tumorigenic remains to be established. An important observation in our study was that a combined inhibition of mTOR and PI3K resulted in a dramatic downregulation of pS6K (Fig. 1G and H). There may be alternative ways by which AKT is regulated by mTORC1 (38). mTORC2 also activates AKT and thus mTOR is at a potential junction to shift AKT levels. Suppression of Rictor but not Raptor by siRNA interference resulted in total inhibition of pAKT expression (Fig. 3C). Due to interacting pathways, mTORC1 activity is dependent on mTORC2. Thus, these findings place mTORC1 regulation downstream of AKT and mTORC2 regulation upstream of AKT.

Activation of p70S6K was influenced by RAPA indicating the ability of mTOR to regulate this kinase. mTOR phosphorylates p70S6K at Thr389 *in vitro* (39), but contrary studies indicate that mTOR mediated Thr389 phosphorylation and p70S6K activation occur via a protein phosphatase 2A dephosphorylation (40). In our study, PDGF- or FN-induced p70S6K^{Thr389} was suppressed by RAPA or LY (Fig. 2A and B). This suggests that p70S6K activation results in increased phosphorylation of ribosomal protein S6K downstream

from it, a key regulator of cell motility and growth. These observations confirm the site of phosphorylation for p70S6K by mTOR in GBM.

Studies have linked mTOR with STAT3 and demonstrated that mTOR activates STAT3 specifically at Ser727 (24). Furthermore, inhibition of mTOR by RAPA inhibits STAT3 activation and glial differentiation (23,33). Recent studies demonstrated that cytokine-induced STAT3 activation was specifically disrupted in PTEN-deficient cells but not PTEN-expressing GBM cells (25). PTEN status of GBM cells exclusively affects pSTAT3^{Ser727} (an mTOR-sensitive site). In fact, increased activation of pSTAT3^{Ser727} correlated with enhanced GBM proliferation (26). Consistent with this study, activation of pSTAT3^{Ser727} by PDGF of FN was totally abolished by pretreatment of GBM cells with LY and RAPA (Fig. 2C and D). Conversely, the total inhibition of cell viability at 48 h by RAPA may be due to inhibition of AKT activation by dephosphorylation, altered localization, and/or inhibition of assembly components. LY or RAPA alone produced minor alterations in Ser727 phosphorylation (data not shown). Our findings suggest that pSTAT3 at the Ser727 site is downstream of mTOR-sensitive proteins and may require intermediate molecule(s) between PI3K and mTOR, perhaps through AKT. Future studies would identify such molecules and may shed light on gliomagenesis since involvement of STAT3 participates in neuronal stem cells regulation (41).

Cell proliferation was suppressed by PI3K or mTOR inhibition. The time treatment of LY showed a time- and dose-dependent suppression of cell growth. RAPA treatment, however, showed a parabolic curve, with decline at 12 h, increase at 24 h, followed by suppression in cell growth at low dose and total inhibition at high dose (48 h) (Fig. 4A and B). Numerous studies have demonstrated that the inhibition of these pathways leads to growth suppression of tumor cells (41). LY or RAPA suppressed PDGF- or FN-induced proliferation (Fig. 4C and D) and combined pre-treatment had an additive effect (Fig. 4E). These observations corroborate with our biochemical findings that a shift from mTORC1 to mTORC2 appears following RAPA treatment.

We observed that radial (non-directional) migration of GBM cells was inhibited by PI3K inhibitor LY but not by RAPA. A marked decline in PDGF-induced migration was seen after the inhibition of both PI3K and mTOR (Fig. 5G). Migration was unaltered by RAPA treatment from 1 to 6 h compared to control; however, a trend towards increased migration from 12 to 24 h was evident (Fig. 5A and B). RAPA has been shown to influence cellular migration in GBM cell line U373 by abrogating F-actin reorganization stimulated by IGF-1 (42). This study also suggested IGF-1 induced phosphorylation of focal adhesion proteins such as FAK, paxillin and p130 via disruption of the mTOR-Raptor complex. Analyzing cell migration can be valuable in assessing gene function and cell behavior of GBM (31). Directional migration using a chemotactic technique showed that migration, while unchanged during early (1 to 3 h) RAPA treatment, resulted in a robust increase in motility at later time points (6, 12 and 24 h) (Fig. 5C and D). This pattern of migration corroborates our biochemical findings where RAPA, while suppressing mTORC1, stimulates mTORC2. Interestingly, cytoskeletal activation downstream from

mTORC2 has been suggested via Rho and other related proteins (16), which are consistent with our observation at a later time point of RAPA induced GBM motility. Alternatively, a study using a transwell two-chamber migration assay indicated that cytokine-induced cell migration did not involve mTOR in cancer cells (43).

Recent studies have demonstrated that mTOR may function via nucleocytoplasmic signaling (44). We observed that stimulation with PDGF influences the cellular localization of mTOR (Fig. 6A). In quiescent GBM cells, PDGF-induced mTOR localization to the nucleus, and this was curtailed by pre-treatment with RAPA. mTOR translocation to the nucleus upon growth factor induction appears to be rapid since it is documented within 30 min of treatment. The exact role of mTOR in the nucleus remains to be explored; however, activated mTOR has been shown to be localized to subnuclear structures that resemble polymorphonuclear (PML) bodies. These PML bodies represent distinct, dynamic structures that control cell proliferation, apoptosis, cellular senescence and are associated with AKT phosphorylation (45).

In conclusion, the frequent activation of AKT in cancer cells and its modulation by mTOR make both of these proteins attractive therapeutic co-targets. As depicted schematically (Fig. 6B), we showed that timed RAPA treatments cause a shift between mTORC1 and mTORC2 from 3 to 6 h, documenting a shift in pS6K and pAKT expression thus influencing proliferation and migration. In order to increase the efficacy of RAPA in controlling GBM dissemination, our results suggest that combined inhibition of mTORC1 and mTORC2 along with PI3K may be effective.

Acknowledgements

We thank Dr Jamoona and Dr Zohrabian for their helpful discussion and Miss Francesca Farinacci and Miss Mera Geis for their technical help. We gratefully acknowledge The American Research Foundation for their support.

References

1. Kallio M, Sankila R, Jaaskelainen J, Karjalainen S and Hakulinen T: A population-based study on the incidence and survival rates of 3857 glioma patients diagnosed from 1953 to 1984. *Cancer* 68: 1394-1400, 1991.
2. Ohgaki H and Kleihues P: Genetic pathways to primary and secondary glioblastoma. *Am J Pathol* 170: 1445-1453, 1991.
3. Wiedemeyer R, Brennan C, Heffernan TP, Xiao Y, Mahoney J, Protopopov A, Zheng H, Bignell G, Furnari F, Cavenee WK, Hahn WC, Ichimura K, Collins VP, Chu GC, Stratton MR, Ligon KL, Futreal PA and Chin L: Feedback circuit among INK4 tumor suppressors constrains human glioblastoma development. *Cancer Cell* 13: 355-364, 2008.
4. Galli R, Binda E, Orfanelli U, Cipelletti B, Gritti A, De Vitis S, Fiocco R, Foroni C, Dimeco F and Vescovi A: Isolation and characterization of tumorigenic, stem-like neural precursors from human glioblastoma. *Cancer Res* 64: 7011-7021, 2004.
5. Holland EC, Hively WP, DePinho RA and Varmus HE: A constitutively active epidermal growth factor receptor cooperates with disruption of G1 cell-cycle arrest pathways to induce glioma-like lesions in mice. *Genes Dev* 12: 3675-3685, 1998.
6. Sanai N, Alvarez-Buylla A and Berger MS: Neural stem cells and the origin of gliomas. *N Engl J Med* 353: 811-822, 2005.
7. Mangiola A, Lama G, Giannitelli C, De Bonis P, Anile C, Lauriola L, La Torre G, Sabatino G, Maira G, Jhanwar-Uniyal M and Sica G: Stem cell marker nestin and c-Jun NH2-terminal kinases in tumor and peritumor areas of glioblastoma multiforme: possible prognostic implications. *Clin Cancer Res* 13: 6970-6977, 2007.

8. Nutt C and Louis DN: *Cancer of Nervous System*. 2nd edition. McGraw-Hill, New York, 2005.
9. Hu X, Pandolfi PP, Li Y, Koutcher JA, Rosenblum M and Holland EC: mTOR promotes survival and astrocytic characteristics induced by Pten/AKT signaling in glioblastoma. *Neoplasia* 7: 356-368, 2005.
10. Groszer M, Erickson R, Scripture-Adams DD, Dougherty JD, Le Belle J, Zack JA, Geschwind DH, Liu X, Kornblum HI and Wu H: PTEN negatively regulates neural stem cell self-renewal by modulating G0-G1 cell cycle entry. *Proc Natl Acad Sci USA* 103: 111-116, 2006.
11. Hay N and Sonenberg N: Upstream and downstream of mTOR. *Genes Dev* 18: 1926-1945, 2004.
12. Phillips HS, Kharbanda S, Chen R, Forrester WF, Soriano RH, Wu TD, Misra A, Nigro JM, Colman H, Soroceanu L, Williams PM, Modrusan Z, Feuerstein BG and Aldape K: Molecular subclasses of high-grade glioma predict prognosis, delineate a pattern of disease progression, and resemble stages in neurogenesis. *Cancer Cell* 9: 157-173, 2006.
13. Holland EC: Gliomagenesis: genetic alterations and mouse models. *Nat Rev Genet* 2: 120-129, 2001.
14. Jacinto E and Hall MN: Tor signalling in bugs, brain and brawn. *Nat Rev Mol Cell Biol* 4: 117-126, 2003.
15. Guertin DA and Sabatini DM: Defining the role of mTOR in cancer. *Cancer Cell* 12: 9-22, 2007.
16. Sabatini DM: mTOR and cancer: insights into a complex relationship. *Nat Rev Cancer* 6: 729-734, 2006.
17. Easton JB, Kurmasheva RT and Houghton PJ: IRS-1: auditing the effectiveness of mTOR inhibitors. *Cancer Cell* 9: 153-155, 2006.
18. Volarevic S and Thomas G: Role of S6 phosphorylation and S6 kinase in cell growth. *Prog Nucleic Acid Res Mol Biol* 65: 101-127, 2001.
19. Reiling JH and Sabatini DM: Stress and mTOR signaling. *Oncogene* 25: 6373-6383, 2006.
20. Dorrello NV, Peschiaroli A, Guardavaccaro D, Colburn NH, Sherman NE and Pagano M: *Science* 314: 467-471, 2006.
21. Harrington LS, Findlay GM, Gray A, Tolkacheva T, Wigfield S, Rebholz H, Barnett J, Leslie NR, Cheng S, Shepherd PR, Gout I, Downes CP and Lamb RF: The TSC1-2 tumor suppressor controls insulin-PI3K signaling via regulation of IRS proteins. *J Cell Biol* 166: 213-223, 2004.
22. Tamburini J, Chapuis N, Bardet V, Park S, Sujobert P, Willems L, Ifrah N, Dreyfus F, Mayeux P, Lacombe C and Bouscary D: Mammalian target of rapamycin (mTOR) inhibition activates phosphatidylinositol 3-kinase/Akt by up-regulating insulin-like growth factor-1 receptor signaling in acute myeloid leukemia: rationale for therapeutic inhibition of both pathways. *Blood* 111: 379-382, 2008.
23. Rajan P and McKay RD: Multiple routes to astrocytic differentiation in the CNS. *J Neurosci* 18: 3620-3629, 1998.
24. Yokogami K, Wakisaka S, Avruch J and Reeves SA: Serine phosphorylation and maximal activation of STAT3 during CNTF signaling is mediated by the rapamycin target mTOR. *Curr Biol* 10: 47-50, 2000.
25. De I, Konopka G, Puram SV, Chan JA, Bachoo RM, You MJ, Levy DE, DePinho RA and Bonni A: Identification of a PTEN-regulated STAT3 brain tumor suppressor pathway. *Genes Dev* 22: 449-462, 2008.
26. Riemenschneider MJ, Betensky RA, Pasedag SM and Louis DN: AKT activation in human glioblastomas enhances proliferation via TSC2 and S6 kinase signaling. *Cancer Res* 66: 5618-5623, 2006.
27. Faivre S, Kroemer G and Raymond E: Current development of mTOR inhibitors as anticancer agents. *Nat Rev Drug Discov* 5: 671-688, 2006.
28. Galanis E, Buckner JC, Maurer MJ, Kreisberg JI, Ballman K, Boni J, Peralba JM, Jenkins RB, Dakhil SR, Morton RF, Jaeckle KA, Scheithauer BW, Dancey J, Hidalgo M and Walsh DJ: Phase II trial of temsirolimus (CCI-779) in recurrent glioblastoma multiforme: a North Central Cancer Treatment Group Study. *J Clin Oncol* 23: 5294-5304, 2005.
29. Chang SM, Wen P, Cloughesy T, Greenberg H, Schiff D, Conrad C, Fink K, Robins HI, De Angelis L, Raizer J, Hess K, Aldape K, Lamborn KR, Kuhn J, Dancey J and Prados MD: Phase II study of CCI-779 in patients with recurrent glioblastoma multiforme. *Invest New Drugs* 23: 357-361, 2005.
30. Fan QW and Weiss WA: Isoform specific inhibitors of PI3 kinase in glioma. *Cell Cycle* 5: 2301-2305, 2006.
31. Berens ME and Beaudry C: Radial monolayer cell migration assay. *Methods Mol Med* 88: 219-224, 2004.
32. Shah OJ, Wang Z and Hunter T: Inappropriate activation of the TSC/Rheb/mTOR/S6K cassette induces IRS1/2 depletion, insulin resistance, and cell survival deficiencies. *Curr Biol* 14: 1650-1656, 2004.
33. Zeng M and Zhou JN: Roles of autophagy and mTOR signaling in neuronal differentiation of mouse neuroblastoma cells. *Cell Signal* 20: 659-665, 2008.
34. Taberero J, Rojo F, Calvo E, Burris H, Judson I, Hazell K, Martinelli E, Cajal S, Jones S, Vidal L, Shand N, Macarulla T, Ramos FJ, Dimitrijevic S, Zoellner U, Tang P, Stumm M, Lane HA, Leibold D and Baselga J: Dose- and schedule-dependent inhibition of the mammalian target of rapamycin pathway with everolimus: a phase I tumor pharmacodynamic study in patients with advanced solid tumors. *J Clin Oncol* 26: 1603-1610, 2008.
35. Rajasekhar VK, Viale A, Socci ND, Wiedmann M, Hu X and Holland EC: Oncogenic Ras and Akt signaling contribute to glioblastoma formation by differential recruitment of existing mRNAs to polysomes. *Mol Cell* 12: 889-901, 2003.
36. Manning BD, Tee AR, Logsdon MN, Blenis J and Cantley LC: Identification of the tuberous sclerosis complex-2 tumor suppressor gene product tuberin as a target of the phosphoinositide 3-kinase/akt pathway. *Mol Cell* 10: 151-162, 2002.
37. Sarbasov DD, Guertin DA, Ali SM and Sabatini DM: Phosphorylation and regulation of Akt/PKB by the rictor-mTOR complex. *Science* 307: 1098-1101, 2005.
38. Kubica N, Crispino JL, Gallagher JW, Kimball SR and Jefferson LS: Activation of the mammalian target of rapamycin complex 1 is both necessary and sufficient to stimulate eukaryotic initiation factor 2Bvarepsilon mRNA translation and protein synthesis. *Int J Biochem Cell Biol* 40: 2522-2533, 2008.
39. Burnett PE, Blackshaw S, Lai MM, Qureshi IA, Burnett AF, Sabatini DM and Snyder SH: Neurabin is a synaptic protein linking p70 S6 kinase and the neuronal cytoskeleton. *Proc Natl Acad Sci USA* 95: 8351-8356, 1998.
40. Peterson RT, Desai BN, Hardwick JS and Schreiber SL: Protein phosphatase 2A interacts with the 70-kDa S6 kinase and is activated by inhibition of FKBP12-rapamycin-associated protein. *Proc Natl Acad Sci USA* 96: 4438-4442, 1999.
41. Morgensztern D and McLeod HL: PI3K/Akt/mTOR pathway as a target for cancer therapy. *Anticancer Drugs* 16: 797-803, 2005.
42. Liu L, Chen L, Chung J and Huang S: Rapamycin inhibits F-actin reorganization and phosphorylation of focal adhesion proteins. *Oncogene* 27: 4998-5010, 2008.
43. Holt RU, Fagerli UM, Baykov V, Ro TB, Hov H, Waage A, Sundan A and Borset M: Hepatocyte growth factor promotes migration of human myeloma cells. *Haematologica* 93: 619-622, 2008.
44. Bachmann RA, Kim JH, Wu AL, Park IH and Chen J: A nuclear transport signal in mammalian target of rapamycin is critical for its cytoplasmic signaling to S6 kinase 1. *J Biol Chem* 281: 7357-7363, 2006.
45. Salomoni P and Pandolfi PP: The role of PML in tumor suppression. *Cell* 108: 165-170, 2002.